Testing of a Gonioreflectometer for Computer Graphics

Hongsong Li
Sing Choong Foo
Kenneth E. Torrance
Stephen H. Westin

TR-PCG-05-01 April 5, 2005

We describe an automated, three-axis BRDF measurement instrument, which can help increase the physical realism of computer graphics renderings by providing light scattering data for the surfaces in a scene. The gonioreflectometer performs rapid measurements of the BRDF of a flat, isotropic, sample surface over the complete visible spectrum and over most of the incident and reflection hemispheres. To validate the instrument, initial measurements were taken and compared with measurements by other instruments. The accuracy of the BRDF measurements is sufficient for computer graphics research, while reciprocity and energy conservation are preserved.

Keywords: Optical instruments, Scattering measurements, Rough surface scattering, Gonioreflectometer, Computer graphics

OCIS codes: 120.4640, 120.5820, 290.5880, 999.9999, 999.9999

1. Introduction

A. Reflectance Acquisition for Computer Graphics

Realistic rendering is that part of computer graphics that strives to simulate the appearance of a three-dimensional scene in the real world. This may replicate the appearance of an actual scene for motion picture special effects or for forensic analysis, or it may predict appearance for evaluation of product or architectural design. Accurate physical simulation is an indispensable component to achieve demonstrably accurate realism, as opposed to a convincing artistic representation.[1,2]

Such simulation differs from most optical simulations in that the output is appearance, rather than quantitative data. Instead of dealing with a single wavelength and/or a single reflection configuration, as is typical in many applications, we must reproduce the directional and spectral dependence of reflectance over the entire angular domain and visible spectrum.

Two major components of the appearance of a surface are wavelength dependence of reflectance (resulting in color) and directional dependence of reflectance (resulting in visual effects such as gloss). Traditional reflectance measurement instruments are ill-suited to acquiring both components.[3-17] Though they can be and have been used to acquire such data, they are usually slow and may be limited in coverage of the wavelength spectrum or the angular domain of reflectance.

The purpose of the current work is to provide an instrument to measure the bidirectional reflectance distribution function (BRDF) for computer graphics. Our instrument is designed especially for

- Broad angular coverage
- High-resolution coverage of the entire visible spectrum
- Rapid operation
- Accuracy sufficient for computer graphics.

B. Previous Work

The special requirements of computer graphics make the design of the gonioreflectometer a real challenge. To render surfaces at arbitrary orientations with arbitrary lighting, we must maximize the coverage of the incident and reflection hemispheres (with highest grazing angles >80°). To render colors accurately, more than 3 spectral samples are required for each angular configuration.[18] In order to fully characterize the angular and spectral distributions of the BRDF for a surface, the total number of samples can easily be 10^4~10^5. Since we need to characterize many surfaces, the measurement operations have to be rapid. The limitations of human vision, such as polarization insensitivity and limited dynamic range, can be exploited to accelerate the process. We now review the relevant previous work in light of our special requirements.

A classic gonioreflectometer includes a light source, a detector, and some means of varying their angles relative to the sample.[3-12] A goniometer is often used to hold and rotate the sample so that the angular configuration can be changed repeatedly to cover the incident and reflection hemispheres. Such instruments can achieve broad angular coverage[3,4] and broadband spectral

coverage.[5,6] But none of these instruments combines these capabilities. For example, Germer et al.[4] have built an instrument (GOSI) that achieves excellent angular coverage, but limited spectral coverage (3 wavelengths) and long measurement time (weeks for a full angular coverage).

To speed acquisition, multiple detectors can be used in parallel. An example of angular parallelism is using a camera, possibly with special optics, to capture thousands of angles at once, as did Ward et al.,[13] Karner et al.,[14] Castonguay,[15] Dana et al.,[16] and Marschner et al.[17] The speed makes such an arrangement popular in the computer graphics community.[13,16,17] Ward et al.[13] introduced an image gonioreflectometer that samples two dimensions of the BRDF (two reflection directions) simultaneously, reducing the measurement time to minutes. On the other hand, a camera is generally unable to provide sufficient accuracy for computer graphics, because of its limited spectral coverage (3 channels) and limited dynamic range (8/12 bits).

To measure across a broad range of individual wavelengths, we could use either a light source selective to wavelength or a detector selective to wavelength. The first option can be a broadband source working with a monochromator or a set of narrow band filters.[6,10] With such an approach, STARR of NIST[6] and the NASA Goddard scatterometer[10] provide high-quality BRDF measurements over the UV-Vis-NIR spectrum. But scanning such a broad spectrum takes a long time (hours for STARR). And these instruments usually cover only a portion of the incident and reflection hemispheres. The second option can be a spectroradiometer that measures the entire spectrum at once,[5] or a narrow-band detector that can vary its wavelength.[13] Feng et al.[5] introduced a gonioreflectometer equipped with a spectroradiometer detector, which

covers a broad range of spectra in one snapshot. Using a spectroradiometer is faster than the first option, though the dynamic range of the measured signals is generally lower.

None of these instruments displays the combination of angular coverage, wavelength resolution, efficiency, and data quality that we desire. To meet our special requirements, we designed and built a gonioreflectometer equipped with a broadband light source rotated about an axis, a goniometric sample stage providing two additional rotational degrees of freedom, a fixed spectroradiometer detector, and a PC control system. The instrument is described in Section 3.

2. Definitions and Nomenclature

The BRDF (Bidirectional Reflectance Distribution Function) is the ratio of the radiance reflected from a surface in the direction (θ_r, ϕ_r) to the irradiance onto the surface from the direction (θ_i, ϕ_i) (see Figure 1).

$$f_r(\theta_i, \phi_i; \theta_r, \phi_r) = \frac{dL_r(\theta_i, \phi_i; \theta_r, \phi_r)}{dE_i(\theta_i, \phi_i)} \tag{1}$$

where θ_i and ϕ_i are the zenith and azimuthal angles of the irradiance, and θ_r and ϕ_r are the zenith and azimuthal angles of the reflected radiance. For an isotropic surface, only three angles are needed. The reflected radiance dL_r and irradiance dE_i have units of W/m^2sr and W/m^2 respectively.

The BRDF satisfies the following rules:

Helmholtz reciprocity:

$$f_r(\theta_r, \phi_r; \theta_i, \phi_i) = f_r(\theta_i, \phi_i; \theta_r, \phi_r) \tag{2}$$

Energy conservation:

$$\int_{\Omega_r} f_r(\theta_i, \phi_i; \theta_r, \phi_r) \cos\theta_r d\Omega_r \leq 1 \tag{3}$$

where the integral is over the reflection hemisphere Ω_r.

We will also use the directional-hemispherical reflectance ρ_{dh}, which is given by the left side of inequality (3). It is the ratio of the radiant power dE_r reflected to the hemisphere to the radiant power dE_i incident onto a surface, both in W/m^2.

$$\rho_{dh}(\theta_i, \phi_i; 2\pi) = \frac{dE_r}{dE_i} \tag{4}$$

3. Description of the Instrument

Our gonioreflectometer consists of four parts: a broadband, high output, stable light source; a positioning mechanism with 3 axes of rotation; a fixed spectroradiometer detector; and a computer system to control the instrument operation, data acquisition, and data processing. An overview of our instrument is shown in Figure 2; the technical parameters for BRDF measurements are listed in Table 1.

This instrument was designed in conformance with the ASTM standard[19] and the special requirements for computer graphics. We chose a tungsten halogen lamp (visible at the upper left corner of Figure 2) for full spectral coverage. At grazing angles of reflection, the detector views a large area on the sample surface, which must be uniformly illuminated. This is achieved with carefully designed light source optics and a large (up to 130mm by 130mm), uniform sample

surface. The light source is mounted on an optical rail of approximately one-meter length, which is attached to a motorized rotation stage. Two more axes of rotation are provided by a goniometric sample holder (near the center of Figure 2), providing the three rotational degrees of freedom needed to sample an isotropic BRDF. To balance spectral coverage, rapid operation, and sufficient dynamic range, we chose to use a high-quality spectroradiometer detector (in the upper right corner of Figure 2), which has a readout spectrum covering the visible range and 16 bits of signal resolution. To speed operations, a PC is used to automatically coordinate all the components of the system. A block diagram of the control system is shown in Figure 3. The laboratory is maintained at 20°C and a relative humidity of 50% to aid sample stability and prevent condensation on the cooled detector.

A. Light Source

The ideal light source for our application would have a nearly uniform emission across the chosen wavelength band (400nm-700nm) and be completely collimated and unpolarized. To approach this ideal, we use the design shown in Figure 4. The light source consists of an MR16 tungsten halogen lamp with integral dichroic reflector (GE ELH, nominal 300W). The light source provides a continuous spectrum in the desired range while minimizing infrared emission, reducing heating of the sample. Such a lamp does exhibit some residual polarization, however, so we use an opal glass diffuser to depolarize the beam. The beam is gathered by an aspheric condenser lens and passed through a small aperture to approximate a point source, and then collimated by a Nikon camera lens (f=135mm) focused at infinity. The source is powered by a regulated, programmable power supply (stable to within 0.03% to give stable output) and cooled

by a fan to avoid deterioration of the dichroic reflector. We normally run the source at 100 volts rather than its rated 120 volts to prolong its life beyond the rated 35 hours.

The resulting beam is well collimated: it subtends a solid angle of approximately 2.4×10^{-5} sr, with illumination uniform to within ±5% over a circular region of 25mm diameter. A scientific grade CCD camera is used to check the uniformity and symmetry of the light spot on the sample surface.

A baffled, ventilated housing around the entire source assembly controls stray light. Control is augmented by the integrated lens hood of the Nikon lens. When needed, we mount a dichroic polarizer on the source arm to control the polarization state of the source; in normal operation we use a depolarized light source.

B. Positioning Mechanism

The sample stage provides two axes of rotation; the third is supplied by moving the source arm in a horizontal plane (parallel to the table). The configuration is similar to that described by Erb and Krystek.[12] All axes are controlled by stepping motors under computer control. All rotational axes intersect at the center of the sample plane, so that measurements at all angles are centered on the same surface point. The sample holder precisely locates the sample plane by means of four supporting lugs, with elastic bands holding the sample with slight pressure from behind. The angular resolution is 0.1° (motors 1 and 2, sample stage) or 0.13° (motor 3, source arm). The maximum angular error is 0.34°, mainly due to backlash in the gear trains of the stages. In most cases, the error is within 0.1°. For BRDF measurements of smooth surfaces,

special procedures are used to reduce the error. All surfaces of the sample holder are painted flat black to minimize stray light scatter.

C. Detector

The detector is designed to accept a broadband signal from the sample, measuring many wavelengths at once for faster operation. The detector unit consists of a folding mirror, focusing optics, and a spectroradiometer (see Figure 2). The position of the entire unit is carefully aligned and fixed. The light scattered by the sample surface is redirected by the folding mirror and focused on the entrance slit of the spectroradiometer through an achromatic doublet. The diffraction grating in the radiometer makes it sensitive to polarization. For this reason, we measure the BRDF twice with different detector polarizations, using a dichroic polarizer in front of the folding mirror to select a single linear polarization for measurement. By averaging the two measurements, and using a detector-polarization calibration curve, we obtain the polarization-averaged reflectance.

Our spectroradiometer consists of two components: a spectrograph with a reflective interference grating of 600 lines/mm and a 1024-pixel diode array detector, covering the visible spectrum (386nm-711nm). We decimate the resolution to 31 output samples (400nm-700nm with 10nm intervals), using a Gaussian kernel, to reduce noise in the output data.

The diode array is thermoelectrically cooled to stabilize its output. The signal resolution is 16 bits. For a fixed exposure time, the dynamic range of the detector is approximately 1:20,000. We verified that the response of the detector, except at very low signal levels, is linear over the

range that we operate the detector. Another experiment confirmed the stability and repeatability of the detector.

The detector optics determine the viewed sample surface area, which is defined by the magnified image of the detector slit on the sample. At θ_r=0° the viewed area is 2mm×4mm; the 2mm dimension increases as $(\cos\theta_r)^{-1}$. The latter represents the fundamental limit on the angular coverage of the instrument: when the projection of the slit exceeds the illuminated spot size, the BRDF will be underestimated. The minimum size of the illuminated spot is 25mm in diameter (for illumination at θ_i=0°), so the constraint on θ_r becomes

$$\theta_{r,\max} = \cos^{-1}\frac{2}{25} \approx 85°$$

The angular limit compares favorably with other computer graphics instruments such as that of Ward et al., which was limited to approximately 60° from the normal.[22]

A typical exposure time is 10 seconds at each angular configuration, resulting in measurement times of roughly 9-10 hours for a reasonably diffuse sample (using about 10^3 angular configurations). The control software automatically senses saturation of the detector and reduces exposure time to obtain useful data in the brightest regions of the BRDF, notably near specular peaks.

D. Control Software

The gonioreflectometer is controlled by a C program that accepts an input file of angular configurations. The file specifies the position of each of the three motors. The program powers

up the light source in a controlled, repeatable fashion, then leads the operator through the steps of aligning the three drive motors, measuring detector dark current, measuring the source intensity, and making two sets of measurements, one for each polarization direction. Subsequently, the operator intervenes only at the start of the measurement to mount the sample, and midway in the measurement process to change the polarizer orientation.

The input file of motor positions is generated offline. For a normal measurement, we generate sampling positions on a regular grid on the unit square. These are then mapped to the unit sphere with a transformation that produces a uniform distribution in solid angle.[23] The transformation from this space to the coordinates of the three stepper motors is reasonably straightforward, and is developed both by Foo[20] and by Erb and Krystek.[12] Some sampling positions (within approximately 7° of retro-reflection) are not achievable, due to mechanical interference between the light source and detector. We omit such positions from the command stream sent to the controller, and depend on later interpolation to fill gaps as needed. Further details of the instrument and operating procedures are available in technical reports.[20,21]

4. Calibrations and Normalization

Once the instrument was built, we calibrated the instrument to yield absolute and relative BRDF measurements. The two methods differ in their calibration and normalization procedures. For both methods, we follow the protocols recommended in the ASTM standard.[19]

A. The Absolute Method

The absolute method of BRDF measurement works from a simple ratio of reflected and incident radiant beams. To do this, we first position the source to illuminate the detector directly, capturing the entire source irradiating flux that impinges on the sample. Subsequently, the reflected flux from the sample is measured at each angular configuration. The spectroradiometric signal for each angular configuration is divided by the signal of the direct light source measurement, the incident cosine, and multiplied by a scale factor K_λ, to give the absolute BRDF value:

$$f_r(\theta_i,\phi_i;\theta_r,\phi_r) = \frac{K_\lambda V_r(\theta_r,\phi_r)}{V_i \cos\theta_i} \tag{5}$$

where K_λ is the calibration factor, which is determined by the configuration of the instrument (it is principally determined by the solid angle of the detector), V_i is the signal of the direct light source measurement, and $V_r(\theta_r,\phi_r)$ is the signal measured by the detector array at λ, θ_r and ϕ_r.

To verify the directional and magnitude accuracy of our instrument, we compare in Figure 5 our polarized BRDF measurements of Spectralon in the incidence plane with data published by Labsphere.[24] The incident light was *p* polarized by installing a horizontal polarizer at the light source. The reflected light of both *s* and *p* polarizations was then measured, at a wavelength of 633nm. The incidence angle was 30° and the reflection angle varied from –86° to 86°. The two sets of *ps* measurements are essentially the same and the *pp* measurements differ slightly (by $0.02 sr^{-1}$). The *pp* measurements include surface scattering that is not present in the depolarized *ps* measurements; we believe that differences in surface finish between our sample and the sample measured by Labsphere account for the differences in the two sets of *ps* measurements.

The absolute normalization method can give good directional and magnitude accuracy for surfaces with strongly specular, or mirror-like, reflection behavior. For such materials, the peak reflected signal may be close in magnitude to the incident source signal. On the other hand, for surfaces with strongly-diffusing reflection behavior, or with very low diffuse reflectance values (dark surfaces), the absolute method can lead to large uncertainties in the measured BRDF values. The uncertainties result because the reflected signal is much smaller than the incident source signal, often by many orders of magnitude, making signal detection difficult. A relative method may be better for such materials.

B. The Relative Method

The relative method of BRDF measurement works by simply comparing the reflected signal from a test sample to that from a reference surface with a known BRDF. To do this, the sample is mounted on the goniometer and the reflected signal is measured for each angular configuration. Subsequently, we measure the reflected signal from the reference sample (Spectralon) at one particular angular configuration, θ_i = 0° and θ_r = 10° (0/10). The spectroradiometric signal from the test sample for each angular configuration is then divided by the signal from the Spectralon at 0/10 and a cosine factor, and multiplied by the absolute BRDF of the Spectralon at 0/10 to give the sample's BRDF:

$$f_r(\theta_i,\phi_i;\theta_r,\phi_r) = \frac{V_{r,sample}(\theta_i,\phi_i;\theta_r,\phi_r)}{V_{r,spectralon}(0,0;10,0)\cdot\cos(\theta_i)} \times f_{r\,spectralon,absolute} \qquad (6)$$

$V_{r,sample}(\theta_i, \phi_i; \theta_r, \phi_r)$ is the spectroradiometric signal from the sample for each angular configuration and $V_{r,spectralon}(0, 0; 10, 0)$ is the spectroradiometric signal from the Spectralon at 0/10. $f_{r,spectralon,absolute}$ is the absolute BRDF of Spectralon at 0/10 derived from measurements of both the angular distribution of the reflected signal by using the gonioreflectometer, and the directional-hemispherical reflectance by using an Optronic Labs OL-750 diffuse reflectometer. Thus, the absolute BRDF of Spectralon at 0/10 becomes the instrument calibration factor.

Our relative method is most similar to the *Relative Total Reflectance Method* recommended in the ASTM standard.[19] That method integrates the measured relative BRDFs over the reflection hemisphere and adjusts calibration factors to match a separately-measured directional-hemispherical reflectance. We use a directional-hemispherical reflectance at only one incidence angle (10°) to obtain the calibration factor. This simplification is valid when the reflectance of the test sample is similar to that of the reference sample in magnitude and directionality. In the next two sections, results obtained using the relative method are presented for three samples.

5. Energy Conservation and Reciprocity

To guarantee that computer-image renderings based on the measured data are physically plausible, we tested energy conservation and reciprocity of the BRDF measurements. In this section, we use a rough aluminum surface to demonstrate the relative method and verify the energy conservation of the BRDF measurements. We tested reciprocity with the Spectralon sample. Similar verification procedures are applied to the other samples and the results are presented in the next section.

A. *Energy Conservation Test*

According to energy conservation, the reflected radiant power to the reflection hemisphere is always less than the incident radiant power onto a surface, as shown in equation (3). The ratio is equal to the integral of the BRDF values over the reflection hemisphere. We tested these rules by measuring a rough aluminum surface, which was prepared by carefully grinding a piece of plate glass with SiC grinding powder of 240 grit, then depositing a pure aluminum coating on the surface. The resulting RMS roughness was 0.63μm.

Figure 6 shows BRDF measurements in the plane of incidence for various illumination angles θ_i. Dense sampling was used in the plane of incidence and the data points are omitted for clarity. The measurements are plausible and consistent with measurements by Torrance and Sparrow.[25] Off-specular peaks beyond the mirror angle of reflection ($\theta_r=\theta_i$) are evident, as is a uniform diffuse (Lambertian) component (to the left in the graph). With increasing incidence angle, the off-specular peak is amplified.

The BRDF was measured over the whole incident and reflection hemispheres. For an incident direction of 10° and a wavelength of 550nm, the BRDF in the reflection hemisphere is shown in Figure 7. The vertical axis is the BRDF; the left and right orthogonal axes map the spherical coordinates above a surface. The plane of incidence corresponds to 0 on the left axis. The sampling positions were uniformly distributed to capture the basically diffuse character of this surface. The points are plotted in a uniform parameterization of the hemisphere such that each grid in the plot represents a region of the hemisphere with the same solid angle. The mapping is responsible for the sharp-edged artifacts along the diagonals; they do not exist in the data.

We tested energy conservation of these measurements by comparing with another instrument. The BRDF data were integrated over the reflection hemisphere according to equations (3) and (4), to obtain the directional-hemispherical reflectance. The same sample was also measured with the Optronics OL-750 diffuse reflectometer system, which obtains the directional-hemispherical reflectance of a flat surface at an incidence angle of 10° with a rated error of less than 1%. Figure 8 shows a comparison of the integrated and direct measurements. In Figure 8, over the entire visible spectrum, the directional-hemispherical reflectance obtained from the gonioreflectometer BRDF measurements is within 2% of the comparison values obtained by direct measurement with the OL-750 system. The only exception is at short wavelengths, below 420nm. At short wavelengths, the tungsten source of the gonioreflectometer has relatively low output, the silicon-based detector has reduced sensitivity, and the dichroic polarizer is much less effective, all of which contribute to the error. The comparison suggests indirectly that the BRDF measurements are accurate in both magnitude and spectrum, with less than 2% integrated error.

B. Reciprocity Test

Equation (2) requires reciprocity; that is, when the positions of the light source and detector are interchanged, the measured results should be the same. To verify reciprocity, the light reflection of Spectralon was measured in the plane of incidence, where $\phi_i=\phi_r=0$. We compared the signal readings of two measurements, each satisfying $\theta_{i1} = \theta_{r2}$ and $\theta_{i2} = \theta_{r1}$. Representative data, shown in Table 2, show that reciprocity is satisfied to within 1% to angles as great as 80° from the surface normal.

6. Measurements and a Rendering Example

In this section, we present measured BRDFs for two additional materials: a metallic silver automotive paint and a glossy yellow paint. In contrast with Section 5, these surfaces represent materials that are more common in typical real-world environments. The silver paint demonstrates the capture of an interesting directional dependence of the BRDF. The silver paint is basically gray in color, as were the materials previously presented. The yellow paint shows our instrument's ability to capture the spectral dependence of the BRDF, resulting in brilliant color. Finally, we demonstrate the utility of our instrument by rendering a realistic image from measured data of an actual sample.

A. Metallic Silver Paint

The metallic silver paint (DuPont) scatters light through a more complex mechanism than the rough aluminum surface considered in section 5A: there is an ideal specular reflection from the smooth, glossy surface of the paint, but most light penetrates the surface and is scattered more diffusely from flakes of metal beneath the surface. Figure 9 shows the measured BRDFs in the plane of incidence. The graph is taken from the full hemispherical data set, so shows coarser sampling than that seen in Figure 6. We have interpolated the sparser data points with a cubic spline (shown with dashed lines) after deleting samples near the specular (mirror) direction to better isolate the subsurface scattering from the first-surface reflection. The deleted mirror peak essentially follows the Fresnel formula for mirror reflection from a smooth dielectric surface. In BRDF coordinates, the mirror peaks would be off scale in Figure 9, and would be centered on the mirror reflection angle with a half angle of about 0.4° due to the small solid angle of the light source.

The paint sample shows a diffuse reflectance pattern in Figure 9 that is very different from the rough aluminum surface (Figure 6). First, there is almost no Lambertian component to the left in the figure. Second, the directional lobe is narrower and is centered on the mirror direction (except for θ_i=80°). Third, the increase in BRDF magnitude with increasing θ_i is much smaller, and reverses as θ_i exceeds 70°. We suspect the third effect is due to two factors: the unknown angular distribution of the subsurface metal flakes, and the first-surface reflection (not shown) which tends to divert a larger proportion of the incident light near grazing incidence.

Figure 10 provides an example BRDF for the paint over the mapped reflection hemisphere, for an incident direction of 10° and a wavelength of 550nm. Figure 11 displays a comparison of the integrated and separately-measured directional-hemispherical reflectances for the paint, over the visible wavelength spectrum. For this figure, the Fresnel component has been excluded from both curves. Figures 10 and 11 respectively resemble their counterparts for the rough aluminum surface, Figures 7 and 8.

B. Glossy Yellow Paint

The glossy yellow paint (Krylon 7221 Canary) scatters light from its surface and from subsurface paint pigments. Reflection from the nearly smooth surface is gloss-like, with Fresnel-like reflection at large angles of incidence. The subsurface scattering is wavelength dependent, giving the material its yellow color, and is diffuse in character.

Figure 12 displays the measured incidence-plane BRDF for three angles of incidence and two wavelengths. The full hemispherical BRDF data set has been interpolated to get the incidence-plane curves. The Fresnel-like mirror component from the surface has been deleted; that component follows the Fresnel formula for mirror reflection from a smooth dielectric and is nearly independent of wavelength since the index of refraction of the paint binder is nearly independent of wavelength. The peaks appearing near the mirror reflection angles of 10º, 40º and 60º are due to a gloss-like component of surface reflection. The gloss peaks vary slightly in magnitude with wavelength. Away from the peaks, there is a nearly constant (i.e., ideal diffuse) BRDF, which arises from the subsurface reflection. Since the subsurface reflection is wavelength dependent, the diffuse component is wavelength dependent.

In comparing the incidence-plane BRDFs for the aluminized ground glass, the metallic paint, and the yellow paint in Figure 6, Figure 9, and Figure 12, respectively, we observe striking differences. The aluminum surface (Figure 6) shows a reflection pattern that is due to first surface reflection from the rough surface (accounting for the reflection peaks) and a nearly constant diffuse pattern that is attributed to multiple reflections among roughness elements on the surface. At larger angles of incidence, the BRDF peaks are at reflection angles beyond the mirror reflection angle. On the other hand, the two paints show strong gloss-like peaks near the mirror reflection angle. For the metallic paint, the peaks arise from metal flakes within the paint binder (Figure 9), whereas for the yellow paint, the peaks arise from a surface glossiness (Figure 12). Further, the metallic paint shows only a weak or nonexistent diffuse reflection away from the gloss-like peaks (Figure 9), whereas the yellow paint shows a strong nearly ideal-diffuse reflection away from the glossy peaks (Figure 12).

For the yellow paint, the BRDF over the mapped reflection hemisphere is sketched in Figure 13 for three incidence angles and three wavelengths. Clearly, the nearly ideal-diffuse reflection component is wavelength dependent, but not strongly incidence-angle dependent. Conversely, the superposed glossy peak is incidence-angle dependent, but not strongly wavelength dependent. Figure 14 provides a comparison of the integrated and separately-measured directional-hemispherical reflectances for the yellow paint, over the visible wavelength range, and the agreement is to within a few percent. For this figure, the Fresnel component has been excluded from both curves.

C. Example Image

Finally, we demonstrate the use of our instrument for its designed purpose by rendering a realistic image of a 3-dimensional scene. We adapted the BRDF measurements of silver paint presented in Section 6A for rendering by approximating them with smooth basis functions.[26] This representation offers both proven accuracy and the computational efficiency needed for rendering, where each BRDF may be evaluated millions of times to generate a single image. Figure 15 was then rendered using Blue Moon Rendering Tools, a RenderMan™-based program that implements high-quality ray tracing.[27] A custom RenderMan™ shader program (available at http://www.graphics.cornell.edu/~westin/lafortune/lafortune.html) was written to implement our BRDF approximation. The car body uses our measured reflectance, with an additional Fresnel term to model reflection from the smooth surface. The convincing appearance of this image demonstrates the usefulness of rendering from actual physical measurements, and the capability of our instrument to provide these measurements.

7. Conclusion

We have presented an automated three-axis gonioreflectometer designed to meet the needs of computer graphics. The instrument can cover almost the entire angular domain of an isotropic BRDF, covers the entire visible spectrum with ample wavelength resolution, and is rapid enough to measure real materials in a practical time (less than ten hours.) The angular range covers the entire incident and reflection hemispheres to an angle of 85°, with the exception of a cone of approximately 7° around retro-reflection. We measure 31 wavelength samples covering the visible spectrum (400nm-700nm) in one snapshot. Our initial measurements have validated the accuracy of the instrument. Computer-generated images based on the measurements are realistic and physically plausible.

As with any instrument, there are future improvements and extensions we would like to make. First, the instrument can be extended to measure anisotropic surfaces by adding a fourth motorized stage to rotate the sample about its normal vector. Second, a beam-splitter arrangement could be added to extract retro-reflection. Finally, use of direct software control opens the possibility of adaptive sampling patterns based on the BRDF as it is measured.

Acknowledgements

The authors would like to thank Professor Donald Greenberg, Hurf Sheldon, and Eric P. F. Lafortune of the Cornell Program of Computer Graphics for their encouragement and technical support. Equipment was donated by the Imaging Science Division of Eastman Kodak (Larry Iwan) and the Hewlett-Packard Company; the silver paint sample was donated by Ford Motor Company. This research was supported by the NSF Science and Technology Center for Computer Graphics and Scientific Visualization (ASC-8920219), by the NSF Thermal Systems Program (CTS-9213183), and by the NSF Information Technology Research Program (ACI-0113851).

References

1. D. P. Greenberg, K. E. Torrance, F. X. Sillion, J. Arvo, J. A. Ferwerda, S. Patanaik, E. P. F. Lafortune, B. Walter, S. C. Foo, and B. Trumbore, "A framework for realistic image synthesis," Comput. Graph. Proc., Annual Conference Series (SIGGRAPH95), 477-494 (1995).
2. X. D. He, K. E. Torrance, F. X. Sillion, and D. P. Greenberg, "A comprehensive physical model for light reflection," *Comput. Graph.* **25** (SIGGRAPH91), 175-186, 1991.
3. L. Davis and J. G. Kepros, "Improved facility for BRDF/BTDF optical scatter measurements," in *Stray Radiation V*, R. P. Breault, ed., Proc. SPIE **675**, 24-32 (1986).
4. T. A. Germer and C. C. Asmail, "A goniometric optical scatter instrument for bi-directional reflectance distribution function measurements with out-of-plane and polarimetry capabilities," in *Scattering and Surface Roughness*, A. A. M. Zu-Hun Gu, ed., Proc. SPIE **3141**, 220-231 (1997).
5. X. Feng, J. R. Schott, and T. Gallagher, "Comparison of methods for generation of absolute reflectance-factor values for bi-directional reflectance-distribution function studies," Appl. Opt. **32**, 1234-1242, 1993.
6. J. E. Proctor and P. V. Barnes, "NIST high accuracy reference reflectometer-spectrophotometer," J. Res. Natl. Inst. Stand. Technol. **101**, 619-627 (1996).
7. J. J. Hsia and J. C. Richmond, "Bidirectional Reflectometry Part I. A high resolution laser bi-directional reflectometer with results on several optical coatings," J. Res. Natl. Inst. Stand. Technol. **80A**, 189-205 (1976).

8. S. Mainguy, M. Olivier, M. Josse, and M. Guidon, “Description and calibration of a fully automated infrared scatterometer,” in *Optical Scatter: Application, Measurement, and Theory*, J. C. Stover, ed., Proc. SPIE **1530**, 269-282 (1991).
9. B. T. McGuckin, D. A. Haner, R. T. Menzies, C. Esproles, and A. M. Brothers, “Directional reflectance characterization facility and measurement methodology,” Appl. Opt. **35**, 4827-4834, 1996.
10. T. F. Schiff, M. W. Knighton, D. J. Wilson, F. M. Cady, J. C. Stover, and J. J. Butler, "Design review of a high-accuracy UV to near-IR scatterometer," in *Optical Scattering: Application, Measurement, and Theory II*, J. C. Stover, ed., Proc. SPIE **1995**, 121-130 (1993).
11. D. R. White, P. Saunders, S. J. Bonsey, J. van de Ven, and H. Edgar, “Reflectometer for measuring the bi-directional reflectance of rough surfaces,” Appl. Opt. **37**, 3450-3454, 1998.
12. W. Erb and M. Krystek, “Ein neuartiges 3D-Gonioreflektometer,” Optik, **83**, 51-54, 1989
13. G. J. Ward, “Measuring and modeling anisotropic reflection,” *Comput. Graph.* **26** (SIGGRAPH92), 265-272, 1992.
14. K. F. Karner, H. Mayer, and M. Gervautz, “Am image based measurement system for anisotropic reflection,” Computer Graphics Forum (Eurographics ’96 Proceedings) **15**, 119-128 (1996).
15. R. J. Castonguay, “New generation high-speed high-resolution hemispherical scatterometer,” in *Optical Scattering: Application, Measurement, and Theory II*, J. C. Stover, ed., Proc. SPIE **1995**, 152-165 (1993).
16. K. Dana, S. Nayar, B. Ginneken, and J. J. Koenderink, “Reflectance and texture of real-world surfaces,” ACM Trans. Graph. **18**, 1-34 (1999).

17. S. R. Marschner, S. H. Westin, E. P. F. Lafortune, and K. E. Torrance, "Image-based bidirectional reflectance distribution function measurement", Appl. Opt. **39**, 2592-2600, 2000.

18. R. A. Hall, "Comparing Spectral Color Computation Methods," IEEE Comput. Graph. Appl. **19**, No.4, 36-45, (1999).

19. American Society for Testing and Materials, *Standard Practice for Angle Resolved Optical Scatter Measurements on Specular or Diffuse Surfaces* (American Society for Testing and Materials, West Conshohocken, PA, 1996), Standard E 1392-96.

20. S. C. Foo, "A gonioreflectometer for measuring the bidirectional reflectance of material for use in illumination computation," M.S. thesis (Cornell University, Ithaca, NY, 1997).

21. H. Li and K. E. Torrance, "Validation of the Gonioreflectometer", Technical Report PCG-03-2 (Program of Computer Graphics, Cornell University, Ithaca, NY, 2003).

22. A. Grynberg and G. Ward, "A new tool for reflectometry," Monograph 161, (Lawrence Berkeley National Laboratory, Berkeley, CA, 1990).

23. P. Shirley and K. Chiu, "Notes on adaptive quadrature on the hemisphere," Technical Report 441 (Department of Computer Science, Indiana University, Bloomington, IN, 1994).

24. A. W. Springsteen, J. Leland and T. M. Ricker, "A guide to reflectance materials and coatings," Labsphere Corporation (North Sutton, NH, 1990).

25. K. E. Torrance and E. M. Sparrow, "Theory for off-specular reflection from roughened surfaces," J. Opt. Soc. Am. **57**, 1105-1114 (1967).

26. E. P. F. Lafortune, S. C. Foo, K. E. Torrance, and D. P. Greenberg, "Non-linear approximation of reflectance functions," Comput. Graph. Proc., Annual Conference Series (SIGGRAPH97), 117-126 (1997).

27. L. Gritz and J. K. Hahn, “BMRT: A global illumination implementation of RenderMan standard,” Journal of Graphics Tools **1**, No.3, 29-47 (1996).

Table 1: Technical Parameters of the Gonioreflectometer

Light Source:	Source Power Drift: 0.03% + 5mA Solid Angle: 2.4×10^{-5} sr
Detector:	Solid Angle: 0.00128sr Signal Readout Resolution: 16 bit Detector Dynamic Range: 1:22,000 Electron Sensitivity: 1,900 photoelectrons/count Spectral Range: 386nm-711nm Spectral Resolution: 2.8nm
Mechanical System:	Rotation Stage 1 Range: 0°~360° Rotation Stage 1 Resolution: 0.01° Rotation Stage 2 Range: 0°~180° Rotation Stage 2 Resolution: 0.01° Rotation Stage 3 Range: 7°~180° Rotation Stage 3 Resolution: 0.013°
Test Sample:	Dimension of Sample Surface: 130mm×130mm Illumination Spot: 25mm diameter Uniformity of Illumination: within ±5% Maximum Angle of Reflection: 85°

Table 2: Reciprocal Measurements on Spectralon with the Gonioreflectometer

θ_i	40	80	46	74	50	70	54	66
θ_r	80	40	74	46	70	50	66	54
Signal Reading	1369	1361	1497	1488	1555	1545	1582	1579
Relative Error	0.58%		0.60%		0.64%		0.19%	

List of Figure Captions:

Figure 1 Coordinate system

Figure 2 Overview of the Gonioreflectometer

Figure 3 Block diagram of the measurement and control system

Figure 4 Light source optical components

Figure 5 Comparison of measured and reference BRDFs for Spectralon in the plane of incidence for θ_i=20°, λ=633nm, and *ps* and *pp* components of polarization

Figure 6 Incidence-plane BRDF of rough aluminum surface for several incidence angles θ_i; λ=550nm

Figure 7 BRDF of rough aluminum over the mapped reflection hemisphere for θ_i =10° and λ=550nm.

Figure 8 Comparison of directional-hemispherical reflectance of rough aluminum as measured by two instruments, θ_i =10°

Figure 9 Incidence-plane BRDF of metallic silver paint for several incidence angles θ_i; λ=550nm

Figure 10: BRDF of metallic silver paint over the mapped reflection hemisphere for θ_i =10° and λ=550nm

Figure 11 Comparison of directional-hemispherical reflectance of metallic silver paint as measured by two instruments, θ_i =10°

Figure 12 Incidence-plane BRDF of glossy yellow paint for several incidence angles θ_i; λ=450, 650nm

Figure 13 BRDF of glossy yellow paint over the mapped reflection hemisphere for various incidence angles and wavelengths

Figure 14 Comparison of directional-hemispherical reflectance of glossy yellow paint as measured by two instruments, θ_i =10°

Figure 15 Computer-generated image based on measured BRDF of the metallic silver paint

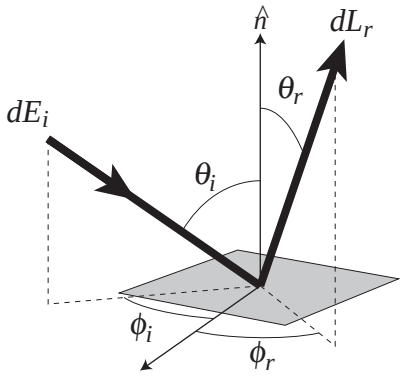

Figure 1 Coordinate system

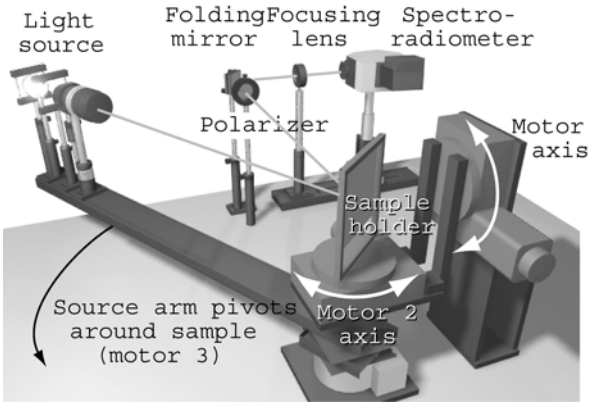

Figure 2 Overview of the Gonioreflectometer

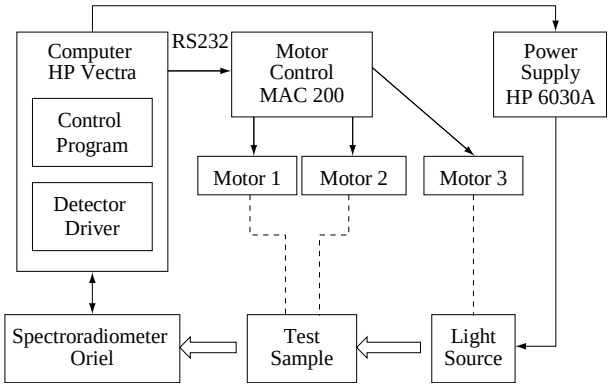

Figure 3 Block diagram of the measurement and control system

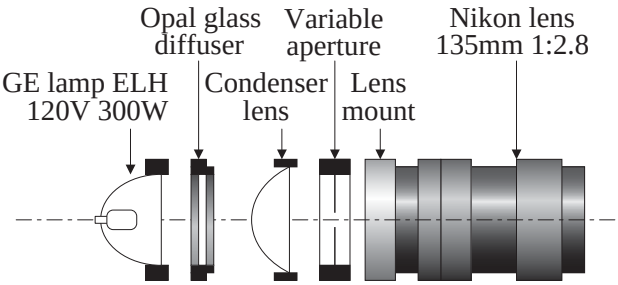

Figure 4 Light source optical components

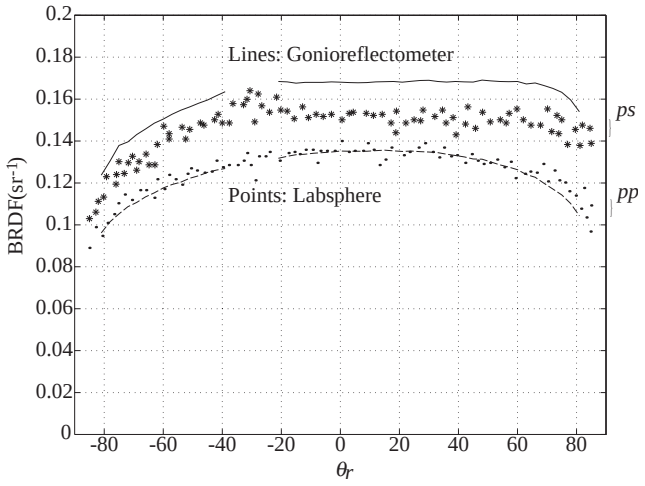

Figure 5 Comparison of measured and reference BRDFs for Spectralon in the plane of incidence for θ_i=20°, λ=633nm, and *ps* and *pp* components of polarization

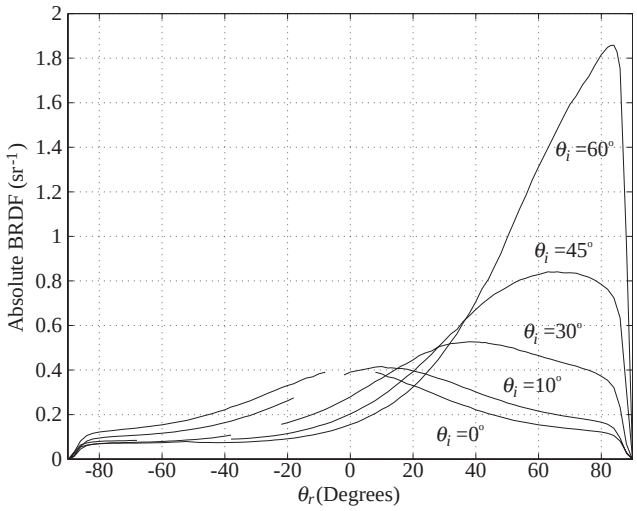

Figure 6 Incidence-plane BRDF of rough aluminum surface for several incidence angles θ_i; λ=550nm

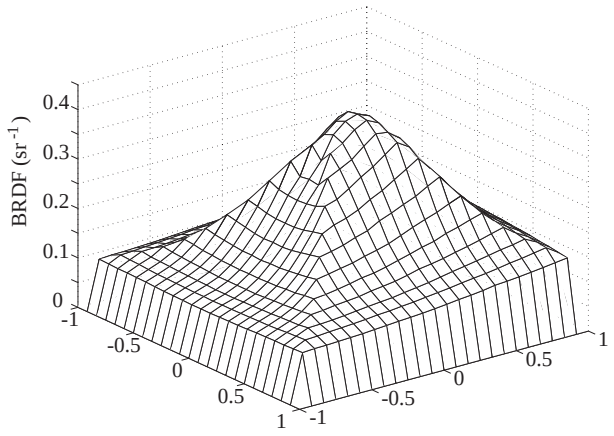

Figure 7 BRDF of rough aluminum over the mapped reflection hemisphere for θ_i =10° and λ=550nm.

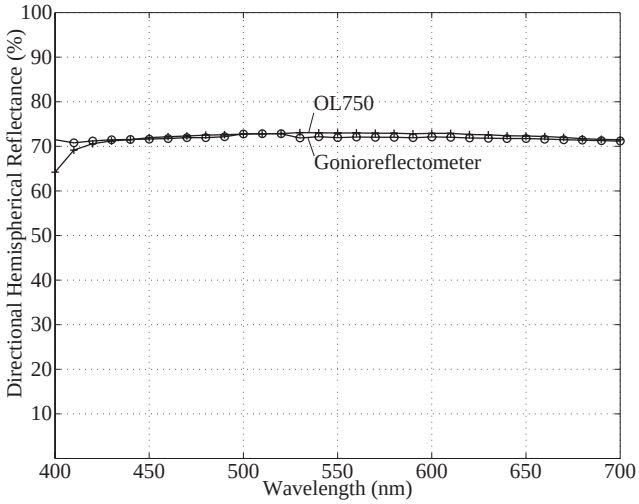

Figure 8 Comparison of directional-hemispherical reflectance of rough aluminum as measured by two instruments, θ_i =10°

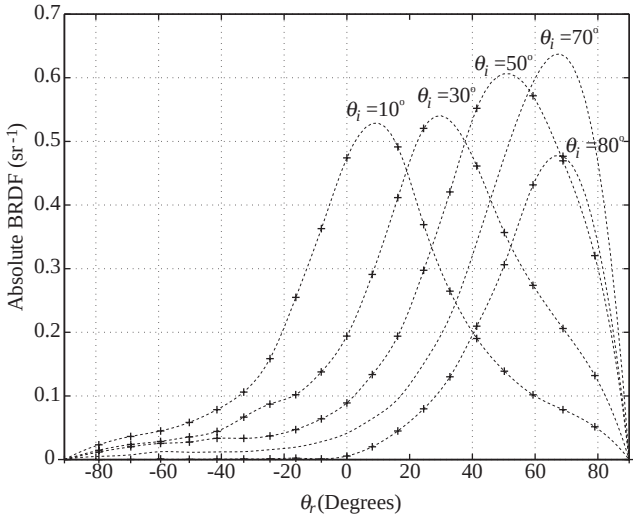

Figure 9 Incidence-plane BRDF of metallic silver paint for several incidence angles θ_i; λ=550nm

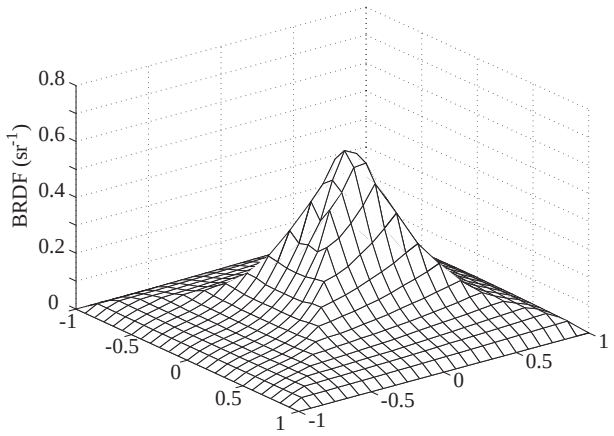

Figure 10: BRDF of metallic silver paint over the mapped reflection hemisphere for θ_i =10° and λ=550nm

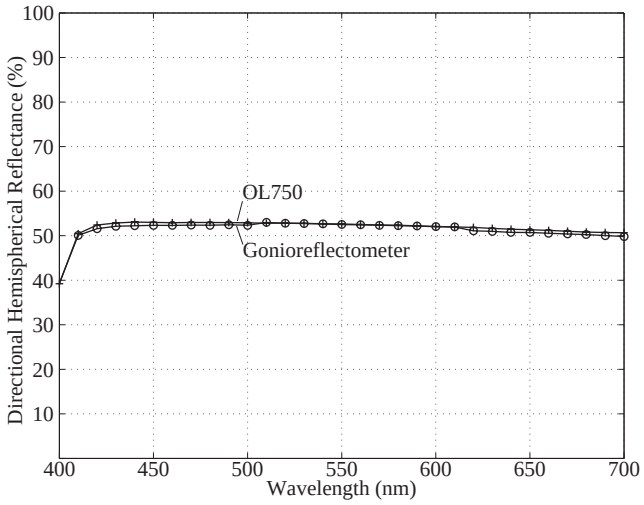

Figure 11 Comparison of directional-hemispherical reflectance of metallic silver paint as measured by two instruments, θ_i =10°

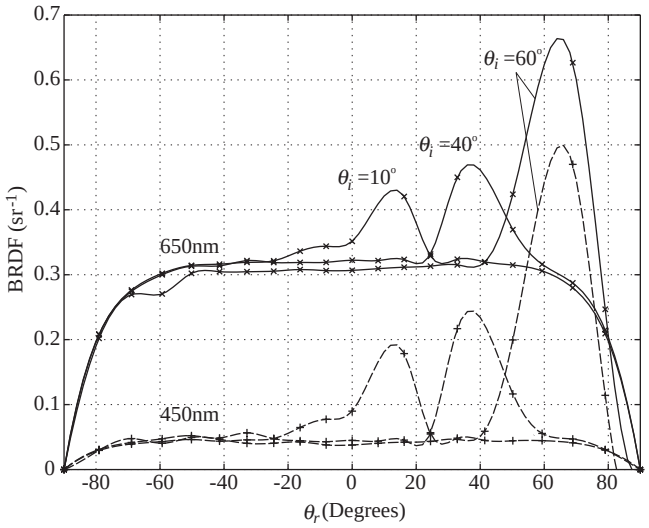

Figure 12 Incidence-plane BRDF of glossy yellow paint for several incidence angles θ_i; λ=450, 650nm

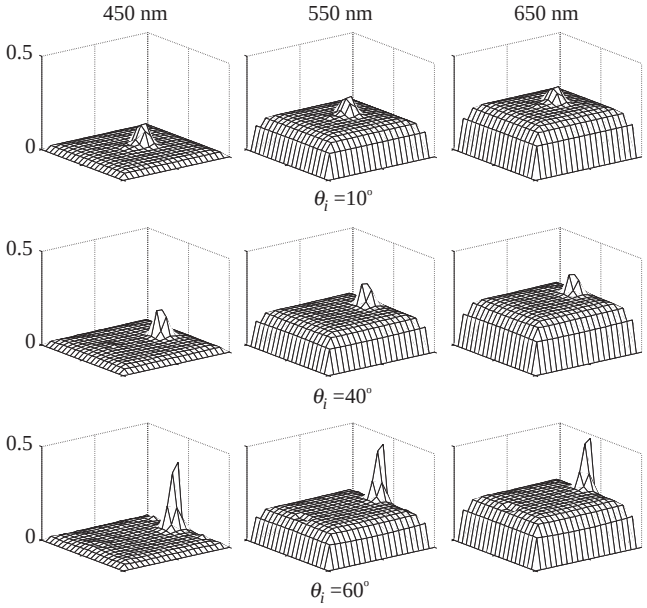

Figure 13 BRDF of glossy yellow paint over the mapped reflection hemisphere for various incidence angles and wavelengths

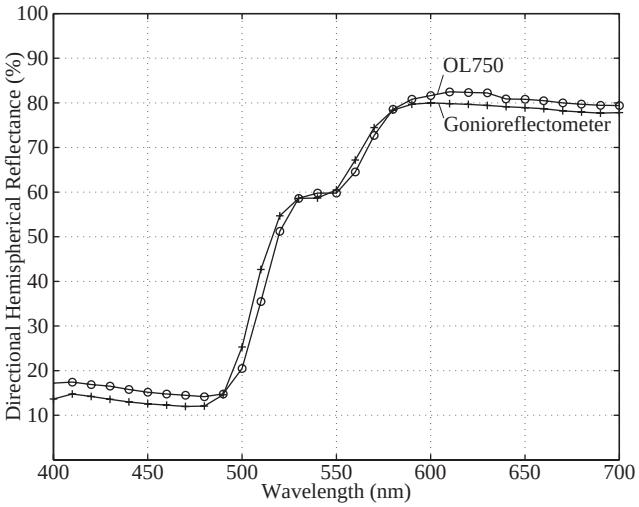

Figure 14 Comparison of directional-hemispherical reflectance of glossy yellow paint as measured by two instruments, θ_i =10°

Figure 15 Computer-generated image based on measured BRDF of the metallic silver paint